Cell Reports, Volume *23*

Supplemental Information

Excess Synaptojanin 1 Contributes to Place Cell Dysfunction and Memory Deficits in the Aging Hippocampus in Three Types of Alzheimer's Disease

Andre M. Miranda, Mathieu Herman, Rong Cheng, Eden Nahmani, Geoffrey Barrett, Elizabeta Micevska, Gaelle Fontaine, Marie-Claude Potier, Elizabeth Head, Frederick A. Schmitt, Ira T. Lott, Ivonne Z. Jiménez-Velázquez, Stylianos E. Antonarakis, Gilbert Di Paolo, Joseph H. Lee, S. Abid Hussaini, and Catherine Marquer

SUPPLEMENTAL FIGURES AND TABLES

Figure S1. Linkage disequilibrium pattern within a haplotype block generated from the familial late onset AD cohort (EFIGA) using SNPs with p-value <0.05, Related to Table 2. Default parameters in Haploview (Barrett et al., 2005) were used.

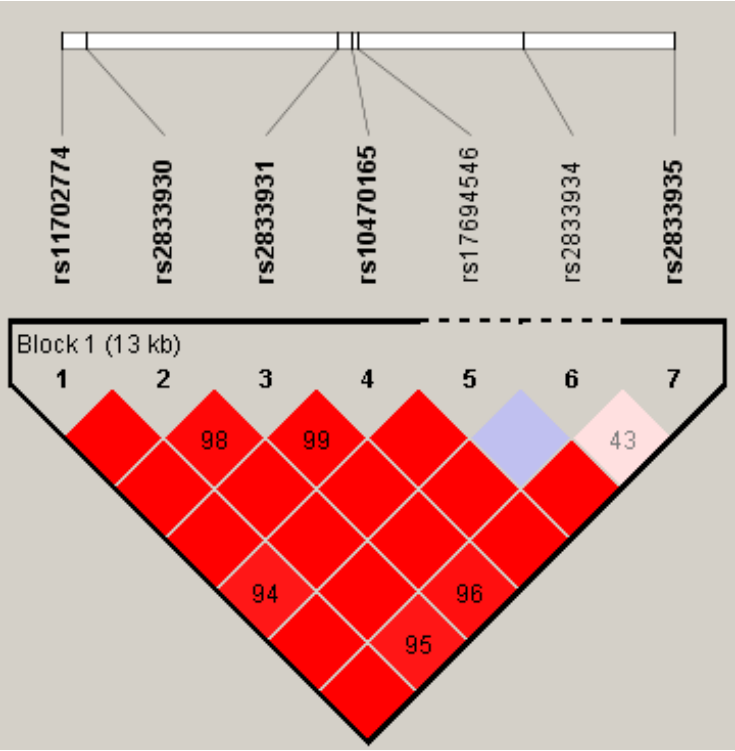

Figure S2. The SNPs identified in *SYNJ1* in the association analysis (Table 1, orange bars) are in linkage disequilibrium (LD) with the eQTLs identified in the GTEx dataset (blue bars), Related to Table 1. In the top part of the figure, the Y1 axis (left, histogram) represent –log p value for genetic association; while the Y2 axis (right, red dots) represent m-values for functional relevance. The linkage disequilibrium (D') patterns between pairwise SNPs were generated using HAPLOVIEW and are presented in the bottom part of the figure. Red squares represent statistically significant LDs; while blue squares represent strong, but not statistically significant, LDs due to small sample size. White squares represent low non-significant LDs.

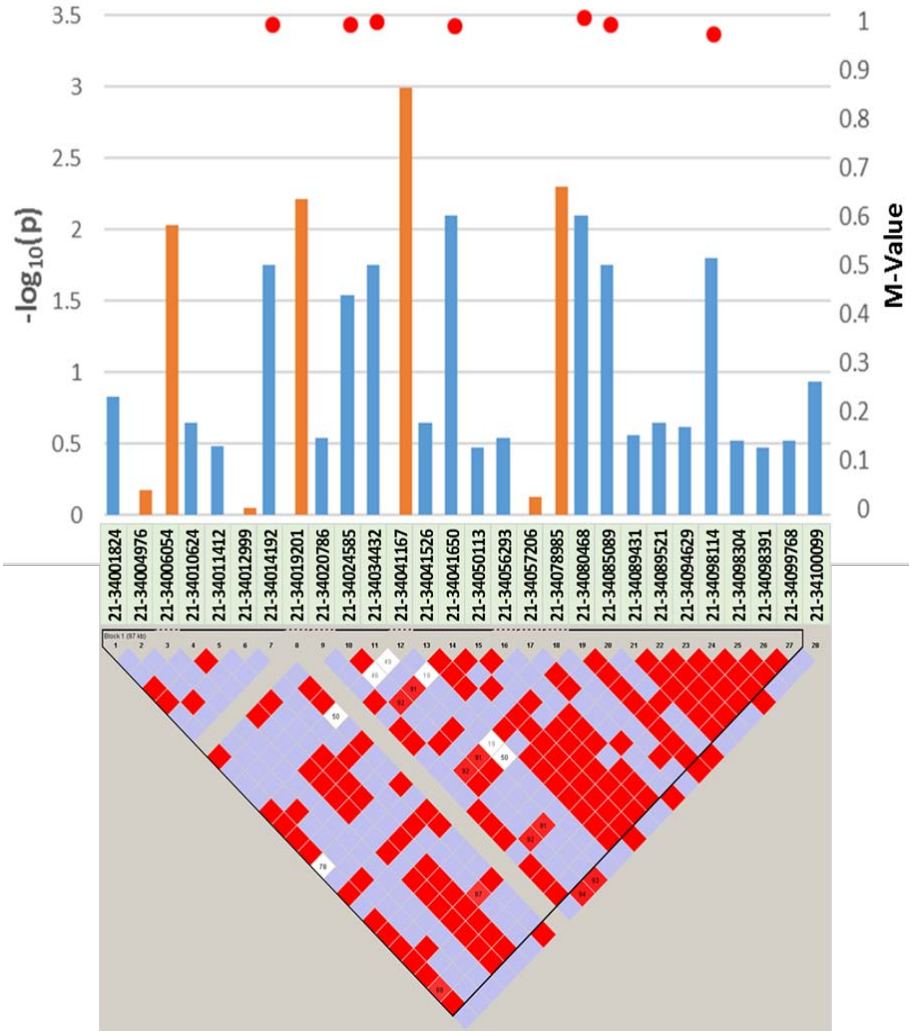

Figure S3. No correlation between SYNJ1 levels and synaptophysin levels in young individuals with DS, Related to Figure 1. Western blot analysis of SYNJ1 and synaptophysin in human post-mortem brain samples from the mid-frontal cortex (BA46) of individuals with DS, aged 1-39 years old (Martin et al., 2014) (n=8). Within this age range, SYNJ1 levels are mildly higher in the DS population (136±47%, n=8), compared to disomic controls (100±12%, n=13), but this difference does not reach significance ($p>0.05$, Student's t-test) (Martin et al., 2014). The line represents the linear regression ($R^2 = 0.28$, $p = 0.178$).

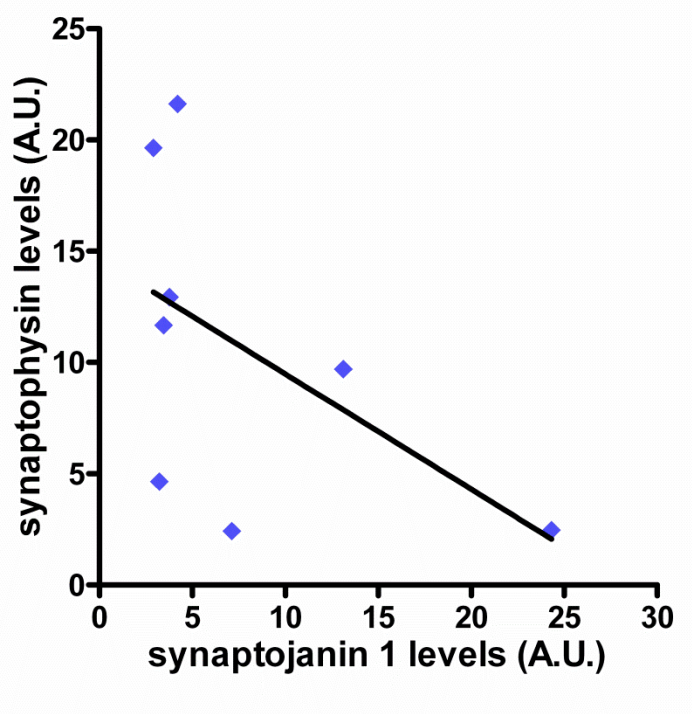

Figure S4. Over-expression of *Synj1* does not affect synaptic protein levels, nor the ability to reach a visible platform, even in older animals, Related to Figure 2. Values denote mean ± S.E.M. (A) Western blot analysis of synaptophysin (SYN) and PSD95 in 19 month-old WT and Tg(*Synj1*) mice (n=4). Tubulin was used as an equal loading marker. Levels of synaptophysin and PSD95 were similar in both genotypes ($p>0.05$ in Student's t-test). (B) Swimming speed (left panel) and latency (right panel) to a visible platform of WT and Tg(*Synj1*) mice. Mice are the same as in Figure 2B and 2C. * denotes $p<0.05$ for the effect of genotype as assessed by two-way ANOVA.

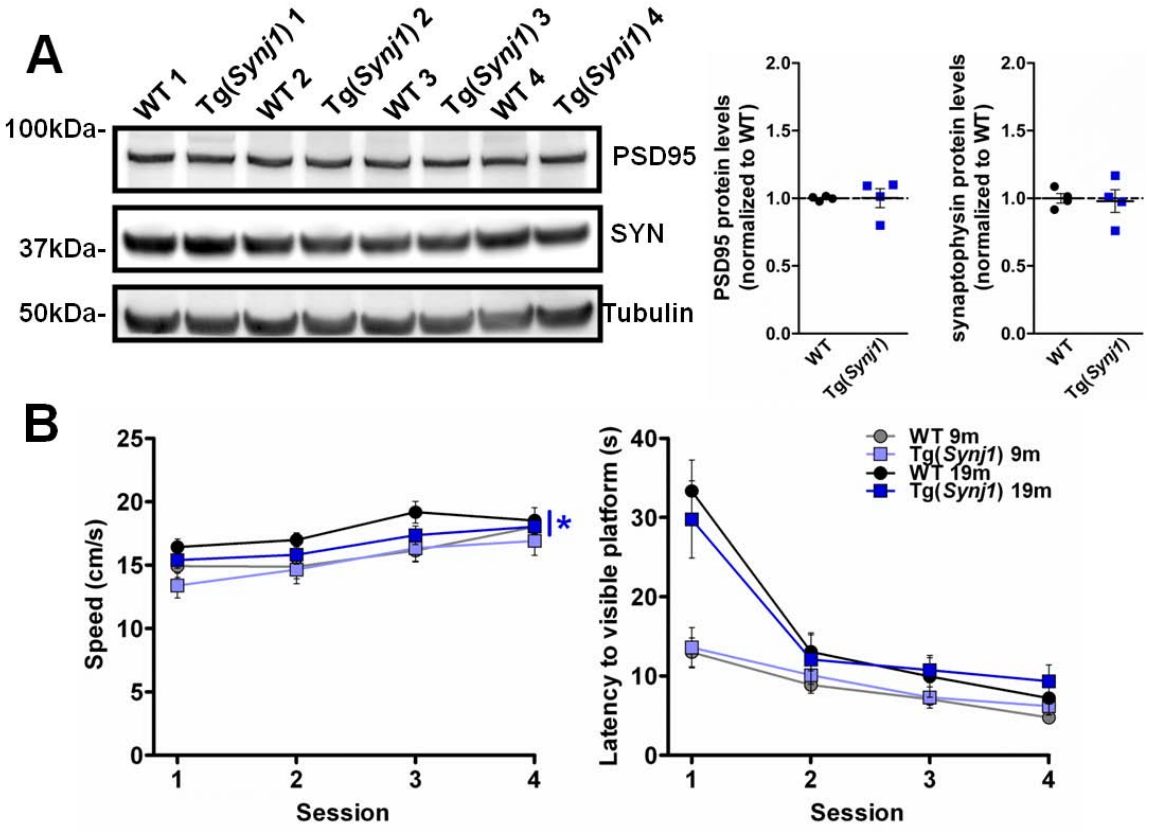

Figure S5. Over-expression of *Synj1* does not affect the firing of inhibitory neurons in the hippocampus, Related to Figure 3. (a) Cresyl violet stained sagittal sections from WT (top) and Tg(*Synj1*) (bottom) animals. Red arrows show electrode trajectories into the hippocampus. (b) Left, the average firing rate of hippocampal interneurons was not significantly altered ($p>0.05$ in Mann Whitney test) in Tg(*Synj1*) (3.4±0.5 Hz, n=36 neurons from 6 animals), compared to controls (4.9±1.1 Hz, n=19 neurons from 5 animals). Right, the peak firing rate of hippocampal interneurons was not significantly altered ($p>0.05$ in Mann Whitney test) in Tg(*Synj1*) (8.2±0.8 Hz, n=36 neurons from 6 animals), compared to controls (9.8±1.6 Hz, n=19 neurons from 5 animals).

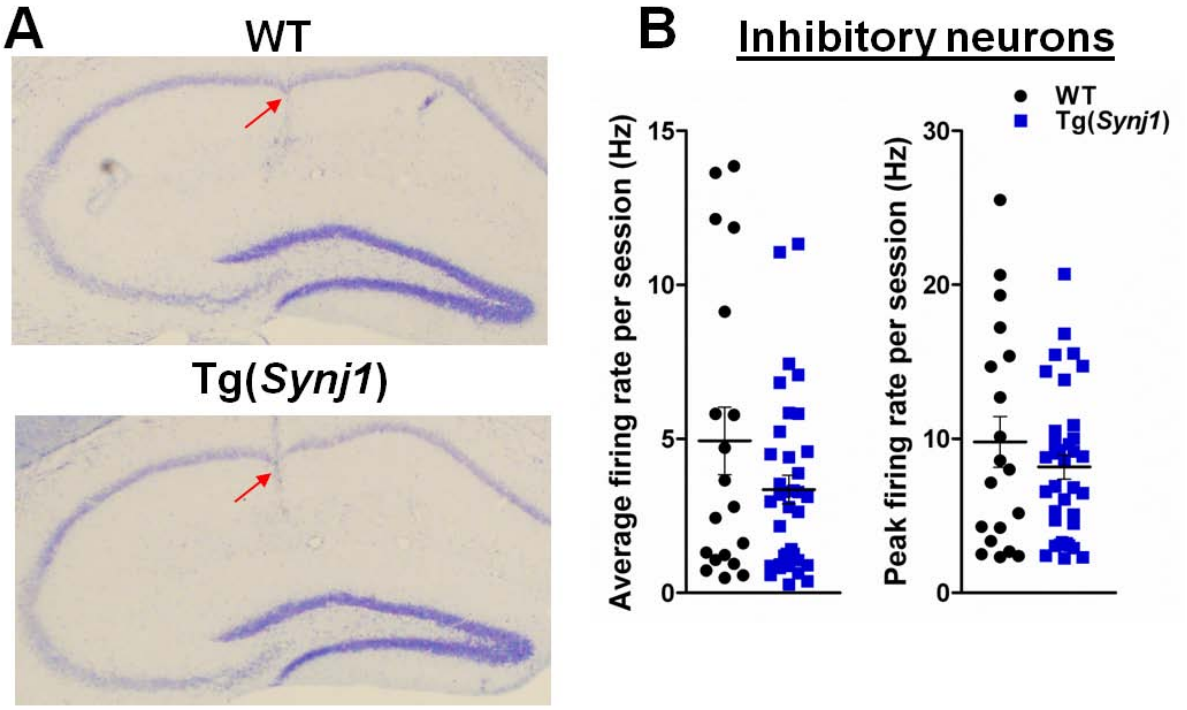

Table S1, Clinical and demographic characteristics of the participating families and their members, Related to Tables 1 and 2. EOAD: early-onset Alzheimer's disease; LOAD: late-onset Alzheimer's disease.

Characteristics	**EOAD**		**LOAD (EFIGA)**	
	Genotyped		**Genotyped**	
	n	**Mean/%**	**n**	**Mean/%**
Familial AD				
Number of families	45		546	
Number of subjects genotyped	305		2199	
Sporadic AD				
Hispanic Sporadic Cases			983	
Hispanic Controls			843	
Affection status				
Affected	74	24.3%	2058	51.1%
Unaffected	231	75.7%	1967	48.9%
Proportion of males: females	132:173	43.3:56.7	1383:2642	34.4:65.6
Age				
Age at onset age (affected)		54.7±7.8		74.4±9.1
Age at last examination (unaffected)		55.5±11.4		67.5±9.3
APOE frequency				
E4	99	16.2%	2206	25.0%
E3	481	78.9%	6216	69.9%
E2	30	4.9%	446	5.1%
G206A Mutation Status				
Carrier	146	47.9%	NA	NA
Non-Carrier	153	50.2%	NA	NA
Unknown	6	2.0%	NA	NA
Education (years)				
Affected	74	11.3±4.5	2058	4.4±4.4
Unaffected	213	12.8±3.8	1967	8.4±5.7
Global Memory (Memory 1)				
Affected	70	8.9±11.4	2058	11.0±10.7
Unaffected	231	34.7±15.4	1967	36.4±9.3
Long-term recall (Memory 2)				
Affected	70	3.4±6.8	2058	5.0±6.4
Unaffected	231	24.0±14.6	1967	24.4±10.7
Delayed recall (Memory 3)				
Affected	70	0.6±1.3	2048	0.9±1.4
Unaffected	230	5.0±3.0	1964	4.8±2.2

Table S2. Gene-wise association analysis for 4 AD-related quantitative traits, Related to Table 1. Bold indicates p<0.05.

Phenotype	N	Number of variants examined in SYNJ1	p-value
Age at onset [(a)]	263	502	**0.0195**
Global memory [(b)]	273	503	0.21499
Long-term recall [(b)]	273	503	**0.04429**
Delayed recall [(b)]	272	500	0.67878

[a] For the age at onset trait, covariates included AD, sex, *PSEN1*-G206A, education, *APOE*4, and principal components (PC1, PC2 and PC3). See text for the definition of age at onset.

[b] For the three memory traits, covariates included age at onset, sex, *PSEN1*-G206A, education, *APOE*4, and principal components (PC1, PC2 and PC3).

Table S3. Multiple genotyping platforms used for the Hispanic GWAS study, Related to Table 2.

STUDY	Microarray SNP chips
Batch 1	Illumina 660k
Batch 2	Illumina 1M
Batch 3	Illumina Omni Express
Batch 4	Infinium OmniExpress
Batch 6	Infinium Global Screening Array
Puerto Rico	Infinium Global Screening Array

SUPPLEMENTAL EXPERIMENTAL PROCEDURES

Differential gene expression in GTEx.

To determine whether variants in *SYNJ1* affect its expression in the brain, we examined the eQTL data (Release V7 (dbGaP Accession phs000424.v7.p2) in the GTEx Portal (https://www.gtexportal.org), restricting our analysis to the 129 tissues in the frontal cortex (BA9) (age range: 20-79 years). Using all variants located within the gene plus those located within 1 MB on either side of the gene, eQTL analysis was performed using the FastQTL algorithm (Ongen et al., 2016), which examines expression levels as a function of SNP dosage, genotype-based principal components, and probabilistic estimation of expression residuals (PEER) (Stegle et al., 2012).

Radial Arm Water Maze (RAWM)

RAWM was performed as described previously (Alamed et al., 2006; McIntire et al., 2012). Briefly, the system consisted of a steel white tank filled with milky water, and containing white walls positioned to produce six arms, radiating from a central area. Spatial cues were present on the walls of the testing room. The location, at the end of one of the arms, of a clear 10 cm plexiglas submerged platform, remained the same for each mouse for the whole duration of the test. On each trial, the mouse started the task from a different randomly chosen arm. Each trial lasted 1 min and errors were counted each time the mouse entered the wrong arm with four paws, or did not take any decision regarding which arm to explore within 10 seconds**.** Each mouse was tested for 15 trials each day for two consecutive days. On the first day, mice were trained for 15 trials, with the first 12 trials alternating between visible (flagged) and hidden (submerged) platform. The last 3 trials of the first day and all of the 15 trials of the second day were performed with a

submerged platform. Results were analyzed by dividing the 30 trials into 10 trial blocks and calculating the average error for each trial block. Tests were performed on 7-9 age-matched mice for each genotype group. All experiments were performed blind with respect to the genotype. Separate tests were performed for males and females. Because no sex-specific differences were found, results from both genders were pooled. Modification of performance with age was quantified by measuring the area under the curve (AUC) for each animal and subtracting [the average AUC for all animals of a given genotype at 9 months] from [the AUC for individual 19 month-old animal of this genotype]. All results were normalized to WT.

Visible platform test

After completing the RAWM experiments, we performed visible platform tests to detect any visual, motor or motivational impairment. These tests were carried out in the same pool but without arms and with a visible (flagged) platform. The platform location was randomly modified to eliminate any contribution of external spatial cues. Mice were given two sessions of three trials each day over 2 days. Each animal was allowed to swim for 1 min from a random location. The time taken (latency) and speed (velocity) to reach the platform were recorded and analyzed using a ceiling-mounted camera, an HVS- 2020 video tracking system and the EthoVision software. Failure to reach the platform was scored as 60 s. Results were analyzed by dividing the 12 trials into 4 trial blocks and calculating an average value for each trial block.

Fear conditioning (FC)

In this paradigm, an innocuous conditioned stimulus (CS), a tone, elicits fear response after being associatively paired with an aversive unconditioned stimulus (US), a foot

shock. The fear response was measured by the frequency of freezing behaviors, which is defined as a stereotyped motionless crouching posture. Contextual and cued FC were performed in a conditioning chamber as previously described (McIntire et al., 2012). Briefly, mice were placed in the conditioning chamber for 2 min before the onset of a discrete tone (CS) (a 30 s sound at 2800 Hz and 85 dB). In the last 2 s of the CS, mice were given a foot shock (US) of 0.50 mA for 2 s through the bars of the floor. After the CS/US pairing, the mice were left in the conditioning chamber for another 30 s and then placed back in their home cages. Freezing behavior was scored using EthoVision software. To evaluate contextual fear learning, freezing was measured for 5 min in the chamber in which the mice were trained 24 hr before the test. To evaluate cued fear conditioning, following contextual testing, the mice were placed in a novel context (cage with smooth flat floor and with vanilla odorant) for 2 min (pre-CS test), after which they were exposed to the CS for 3 min (CS test), and freezing was measured. Tests were performed on 6-14 age-matched mice for each genotype group. All experiments were performed blind with respect to the genotype. Separate tests were performed for males and females. Because no sex-specific differences were found, results from both genders were pooled.

Murine brain tissue preparation and western blot

Mice were anesthetized with ketamine and xylazine (100 and 10 $mg.ml^{-1}$, respectively) and transcardially perfused with saline. Hippocampi were dissected, flash-frozen in liquid nitrogen and kept at -80°C for western blot analysis. Frozen regions were weighed and homogenized in 10 volumes of RIPA buffer (Thermo Fisher) using a microtube homogenizer (VWR). The resulting suspension was then centrifuged at 16,000 g for 15

min. Total protein content was estimated with BCA Protein assay kit (Thermo Fisher). Normalized samples, with the exception of the ones used for synaptojanin 1, were boiled for 10 min at 95 °C in 2x LDS sample buffer (Thermo Fisher) and 10x Sample Reducing Agent (Thermo Fisher). SDS–PAGE was performed on samples (30 μg total proteins) loaded in NuPAGE 4–12% Bis-Tris gels (Thermo Fisher). Wet transfer was performed at 80V for 105 min at 4 °C in Tris-glycine 0.5%-SDS (Boston Bioproducts). Primary and secondary antibodies were incubated overnight at 4 °C and 60 min at room temperature, respectively. Western blot analysis was performed with antibodies raised against Synaptojanin 1 (1:5000, 145 003, SynapticSystems), PSD95 (1:2,000, 51-6900, Thermo Fisher) and synaptophysin (1:2,000, SY38, Millipore). Tubulin (1:10,000, T5168, Sigma) was used for normalization. Peroxidase-conjugated secondary antibodies were from Biorad and were used at a dilution of 1:3,000 (1:10,000 for tubulin). Revelation was performed with Immobilon Western Chemiluminescent HRP Substrate (EMD Millipore) and the chemiluminescent signal was imaged with ImageQuant LAS4000 mini (GE Healthcare). Quantification was performed with ImageJ. At least 4 mice of each genotype were used and each group was gender-matched.

Electrode implantation and surgery

Custom-made, reusable 16-channel microdrives (Axona, UK) were constructed as described previously (Hussaini et al., 2011) by attaching an inner (23 ga) and an outer (19 ga) stainless steel cannula to the microdrives. Tetrodes were built by twisting four 25 mm thick platinum-iridium wires (California wires) and heat bonding them. Four such tetrodes were inserted into the inner cannula of the microdrive and connected to the wires of the microdrive. One day prior to surgery, tetrodes were cut to an appropriate length

and plated with a platinum solution until the impedance dropped to about 150 kOhms. On the day of surgery, mice were anesthetized with either a mixture of ketamine (100 mg/kg) and xylazine (10 mg/kg) or with 1-5% isoflurane mixed with oxygen. Mice were then fixed within the stereotaxic frame with the use of zygomatic process cuff holders. An incision was made to expose the skull and about 3-4 jeweler's screws were inserted into the skull to support the microdrive implant. An additional screw connected with wire was also inserted into the skull and served as a ground/reference for EEG recordings. A 2 mm hole was made on the skull at coordinates 1.8 mm ML and 1.8 AP from bregma. Tetrodes were then lowered to about 0.9 mm from the surface of the brain. Dental cement was spread across the exposed skull and secured with the microdrive. Mice were allowed to recover from anesthesia in a clean cage placed on a warm heating pad until awake (~15 min) before being transported to housing. Carprofen (5 mg/kg) was administered to mice prior to surgery and post-operatively to reduce pain. Mice usually recovered within 24 h, after which the tetrodes were lowered and recording begun. Both male and female mice were used. At least five 24-month old mice of each genotype were used.

In vivo recording and place cell analysis

Mice explored a white box (50 x 50 cm) or a white cylinder (dia. 50 cm). All mice underwent two recording sessions of 10-20 minutes per day, with ≥ 4 hr between sessions. Only sessions with similar coverage (>30%) were analyzed across groups. Tetrode positions were not moved more than 50 μm at a time, and only after the last recording session of the day, allowing > 12 hr of stable electrode positioning prior to the next recording session. All mice included in our study underwent ≥ 16 recording sessions. Neuronal signals from experimental mice were recorded using the Axona

DaqUSB system. Signals were amplified 15,000 to 30,000 times and band-pass filtered between 0.8 and 6.7 kHz. EEG was recorded from 4 channels of the electrodes. EEG was amplified 15,000 times, low-pass filtered at 500 Hz and sampled at 4,800 Hz. Notch filter was used to eliminate 60 Hz noise. The recording system tracked the position of the infrared LED on the head stage (sampling rate 50 Hz) by means of an overhead video camera. Position data were speed-filtered and only speeds of 3 cm/s or more were included. Tracking artifacts were removed by deleting samples greater than 100 cm/s and missing positions were interpolated with total durations less than 1 s, and then smoothing the path with a 21- sample boxcar window filter (400 ms; 10 samples on each side). Spike sorting was performed offline using TINT cluster-cutting software and Klustakwik automated clustering tool. The resulting clusters were further refined manually and validated using autocorrelation and cross-correlation functions as additional separation tools. Quantitative measurements of cluster quality was subsequently performed, yielding isolation distances in Mahalanobis space (Schmitzer-Torbert et al., 2005).

The place cells were separated from inhibitory interneurons based on the spike width (> 300μs) and firing rate (< 30Hz). To ensure that we recorded from the same place cell across sessions, we confirmed that the properties such as autocorrelation, waveform, firing rate and firing location were similar in both sessions. The inhibitory interneurons were easily identified by their high frequency of firing with narrow waveform width and place nonspecific firing. Each sorted place cell was visualized by plotting its firing rate on top of an animal's walking path, with heat map colors ranging from blue (little or no firing) to red (high firing rate). A normalized firing rate map was obtained by dividing the spiking activity with the animal's position at a particular place. Firing rate maps were

smoothed with a filter such that 1 cm equaled 2 pixels. Peak firing was the maximum amount of firing by a cell in a particular session and average firing was calculated by dividing total spikes with total time in a session. Place field size was measured as in previous studies (Muller et al., 1987). Briefly, we calculated the number of pixels inside the enclosure where place cells fired normalized with the number of pixels the mice visited. Only the top 80% of the firing peak with at least 8 contiguous pixels was used and defined as the place field. Only the largest place field was used for place field analysis. Spatial coherence estimates smoothness of a place field. It was calculated by correlating the firing rate in each pixel with firing rates averaged with its neighboring 8 pixels. It measures the extent to which the firing rate in a pixel is predicted by the rates in its neighbors (Muller and Kubie, 1989). Abrupt changes in firing rates of neighboring pixels make the placefields incoherent. Spatial information content is a measure used to predict the location of an animal from the firing of a cell. Information content was calculated using Skaggs' formula (Markus et al., 1994; Skaggs et al., 1993) and measures the amount of information carried by a single spike about the location of the animal and is expressed as bits per spike:

$$Spatial\ information\ content = \sum Pi\left(\frac{Ri}{R}\right) log2\left(\frac{Ri}{R}\right)$$

where i is the bin/pixel number, Pi is the probability for occupancy of bin i, Ri is the mean firing rate for bin/pixel i and R is the overall firing mean rate. Spatial coherence and information content from session 1 were compared with measures from session 2. The reproducibility or stability of place fields is a good measure of animal's memory of space across time. It was calculated by performing a Pearson's product moment correlation on

two firing map fields across two consecutive sessions. Only regions covered by the animal in both sessions were compared and analyzed. The correlation formula is given by:

$$r = \frac{1}{n-1} \sum_{i=1}^{n} \left[\left(\frac{Xi - \bar{X}}{\sigma x} \right) \left(\frac{Yi - \bar{Y}}{\sigma y} \right) \right]$$

where $\frac{Xi - \bar{X}}{\sigma x}, \bar{X}$ and σx are the standard score, sample mean, and sample standard deviation of data X, respectively.

Histology

To determine the exact position of the tetrodes in the brain, mice were anesthetized with an overdose of 0.5 ml ketamine and xylazine solution (100 mg/kg and 10 mg/kg, respectively) and perfused with 4% PFA solution, following which the tetrodes were moved up and the mice decapitated. The brain was gently removed and stored in 4% PFA solution for 24 hr. It was then placed in a 30% sucrose solution for 48–72 hr and was coronally sliced in 30 μm thick sections using a cryostat. The sections were stained with cresyl violet and mounted onto a slide. The brain sections were viewed under a light microscope and digital pictures of the slices acquired. The tips of the tetrodes were identified visually and marked with red arrows.

SUPPLEMENTAL REFERENCES

Alamed, J., Wilcock, D.M., Diamond, D.M., Gordon, M.N., and Morgan, D. (2006). Two-day radial-arm water maze learning and memory task; robust resolution of amyloid-related memory deficits in transgenic mice. Nature protocols *1*, 1671-1679.

Barrett, J.C., Fry, B., Maller, J., and Daly, M.J. (2005). Haploview: analysis and visualization of LD and haplotype maps. Bioinformatics *21*, 263-265.

Hussaini, S.A., Kempadoo, K.A., Thuault, S.J., Siegelbaum, S.A., and Kandel, E.R. (2011). Increased size and stability of CA1 and CA3 place fields in HCN1 knockout mice. Neuron *72*, 643-653.

Markus, E.J., Barnes, C.A., Mcnaughton, B.L., Gladden, V.L., and Skaggs, W.E. (1994). Spatial Information-Content and Reliability of Hippocampal Ca1 Neurons - Effects of Visual Input. Hippocampus *4*, 410-421.

Martin, S.B., Dowling, A.L.S., Lianekhammy, J., Lott, I.T., Doran, E., Murphy, M.P., Beckett, T.L., Schmitt, F.A., and Head, E. (2014). Synaptophysin and Synaptojanin-1 in Down Syndrome are Differentially Affected by Alzheimer's Disease. J Alzheimers Dis *42*, 767-775.

McIntire, L.B., Berman, D.E., Myaeng, J., Staniszewski, A., Arancio, O., Di Paolo, G., and Kim, T.W. (2012). Reduction of synaptojanin 1 ameliorates synaptic and behavioral impairments in a mouse model of Alzheimer's disease. The Journal of neuroscience : the official journal of the Society for Neuroscience *32*, 15271-15276.

Muller, R.U., and Kubie, J.L. (1989). The Firing of Hippocampal Place Cells Predicts the Future Position of Freely Moving Rats. Journal of Neuroscience *9*, 4101-4110.

Muller, R.U., Kubie, J.L., and Ranck, J.B., Jr. (1987). Spatial firing patterns of hippocampal complex-spike cells in a fixed environment. The Journal of neuroscience : the official journal of the Society for Neuroscience *7*, 1935-1950.

Ongen, H., Buil, A., Brown, A.A., Dermitzakis, E.T., and Delaneau, O. (2016). Fast and efficient QTL mapper for thousands of molecular phenotypes. Bioinformatics *32*, 1479-1485.

Schmitzer-Torbert, N., Jackson, J., Henze, D., Harris, K., and Redish, A.D. (2005). Quantitative measures of cluster quality for use in extracellular recordings. Neuroscience *131*, 1-11.

Skaggs, W.E., McNaughton, B.L., Gothard, K.M., and Markus, E.J. (1993). An information-theoretic approach to deciphering the hippocampal code. Advances in Neural Processing Systems *5*, 1030-1037.

Stegle, O., Parts, L., Piipari, M., Winn, J., and Durbin, R. (2012). Using probabilistic estimation of expression residuals (PEER) to obtain increased power and interpretability of gene expression analyses. Nature protocols *7*, 500-507.